KUFA JOURNAL OF ENGINEERING
ISSN 2071-5528
PRINTED IN IRAQ

Volume 3, Number 2 pp.115- 132 , 2012

ANALYSIS OF PILED-RAFT FOUNDATION BY THE FINITE ELEMENT METHOD

Dr.Omar al-Farouk Salem al-Damluji
Former Professor,
Department of Civil Engineering,
College of Engineering,
University of Baghdad, Iraq.

Nadher Hassan Al-Baghdadi
Assistant Lecturer,
Department of Civil Engineering,
College of Engineering,
University of Kufa, Iraq.

(Received:22/9/2011 ; Accepted :22/2/2012)

ABSTRACT

The piled raft is a geotechnical composite construction consisting of three elements: piles, raft and soil. It is suitable as a foundation for large buildings. This paper presents an analysis of piled raft foundation, included material nonlinearity and soil structure interaction. An efficient computer program in FORTRAN 90is developed for this analysis. A 20 node disoparametric brick element has been used to model pile, raft, soil and interface materials. Thin layer interface element has been used to model the contact zone between the pile and soil, and between raft and soil. The behavior of the piled raft material is simulated by using a linear elastic model. However, the behavior of soil and interface materials is simulated by an elasto-plastic model by the use of Mohr-Coulomb failure criterion. Some of the variables of piled-raft system, related to settlement and differential settlement in sandy soil, have been studied, where the length of piles and distance between piles an effective role in reducing both settlement and differential settlement of foundation system. Also increasing the thickness of raft foundation reduces the effectiveness of additional piles for the purpose of reducing differential settlement.

تحليل الأسس الحصيرية المرتكزة على ركائز بطريقة العناصر المحددة

د.عمر الفاروق سالم الدملوجي
الأستاذ الأسبق
كلية الهندسة ، جامعة بغداد

ناظر حسن البغدادي
مدرس مساعد،
كلية الهندسة ، جامعة الكوفة

الخلاصة:

عندما تضاف الركائز العمودية إلى الأسس الحصيرية يتكون منشأ ذو انشاء مركب يتكون من الاساس الحصيري نفسه والركائز وكذلك التربة. يكون هذا النوع من الأسس مناسبا للابنيه ذات الارتفاع العالي.لقد تمت صناعة برنامج عناصر محدده لحل المسائل اللاخطيه ذات ثلاثة أبعاد لحل منظومة الأسس الحصيرية المستندة على ركائز عمودية وذلك بأستخدام لغة فورتران (FORTRAN 90). لقد تم توظيف عنصر طابوقي (Brick Element) ذو عشرين عقده لتمثيل مادة الاساس الحصيري و مادة الركائز ومادة التربة و كذلك العنصر البيني(Interface Element). تم استعمال العنصر البيني ذو الطبقة الرقيقة (Thin Layer Interface Element)لتمثيل منطقة التلامس بين الاساس الحصيري والتربة وكذلك بين الركائز والتربة. تم اعتبار تصرف مادة الاساس الحصيري وكذلك الركائز مرنا خطيا (Linear Elastic)، في حين تم اعتبار سلوك التربة والعنصر البيني سلوكا مرنا لدنا (Elasto-Plastic) باستعمال معيار فشل مور كولومب (Mohr-Coulomb Failure Criterion). تم التحقق من النتائج المحتسبة من البرامجيات وذلك بمقارنتها مع نتائج حقلية من بحوث اخرى، بصورة عامة لقد كانت النتائج متوافقة مع المشاهدات الحقلية. تمت دراسة بعض المتغيرات التي تخص الهبوط والهبوط التفاضلي لمنظومة الاساس في التربة الرملية حيث كان لطول الركائز وكذلك المسافة بين الركائز دورا فاعلا في تقليل الهبوط الكلي و التفاضلي للاساس الحصيري. كذلك فان زيادة سمك الاساس الحصيري يقلل من فاعلية اضافة الركائز للاساس الحصيري لغرض تقليل الهبوط التفاضلي.

1.Introduction:

A piled raft foundation is a geotechnical composite construction consisting of three elements: piles, raft, and subsoil.In comparison with conventional foundation design, a piled raft foundation exhibits a totally new dimension for subsoil-structure interaction because of the new design philosophy as to use the piles up to their ultimate bearing capacity regarding the soil-pile interaction. Another difference from traditional foundation design where the load is assumed to be carried either by the raft or by the piles, the total superstructure load is partly taken by the raft through contact with soil and the remaining load is taken by piles through skin friction. The piles in this case do not have to penetrate to fill depth of soil layer, but it can be terminated at lower depths. This lead to an extremely economic foundations. The concept of piled raft foundation has been described by several authors including Zeevaert (1957), Davis and Poulos (1972), Hooper (1973), Burland et al (1977), Brown and Wiesner(1975), Sommer et al (1985), Price and Wardle (1986), Franke (1991), Hansbo (1993) and Franke et al (1994) among many authors.

2. Equilibrium Equation for Nonlinear Continuum:

The governing equilibrium equation for a nonlinear continuum in elastic equilibrium will be derived using the principle of virtual work.

$$\delta W_{ext} = \delta W_{\text{int}} \quad \textbf{(1)}$$

Where, $\boldsymbol{\delta W_{ext}}$the virtual work due to external action, and

$\boldsymbol{\delta W_{int}}$ the virtual strain energy due to internal stress.

The external work done during moving the body surface **{b}** and surface traction **{t}** through the virtual displacement ∂**{u}** is(Timoshenko and Goodier, 1951):

$$\int \delta W_{ext} = \int_V \partial\{u\}^T \{b\} dV + \int_S \partial\{u\}^T \{t\} dS \quad \textbf{(2)}$$

where, **V** is the volume of the body, and

S is the surface of the body where the external tractions are prescribed.

3. Finite Element Formulation:

In this paper, twenty-noded quadratic hexahedral element of serendipity type has been adopted for the modeling of soil, pile, raft and interface. The equilibrium equation for an element has been obtained using the *principle of virtual work*(Zienkiewicz, 1971):

$$\sum_n \int_V [B]^T [D][B] dV^e \{u\}^e - \sum_n \int_{V^e} [N]^T \{b\}^e dV^e - \sum_n \int_{S^e} [N]^T \{t\}^e dS^e = 0 \quad \textbf{(3)}$$

The equilibrium equation for the complete structure has been obtained after assembling the equilibrium equations of all elements in the structure (Zienkiewicz, 1971).

4. Constitutive Models:

According to Mohr-Coulomb criterion the shear strength increases with the increasing normal stress on failure plane.

$$\tau = c + \sigma \tan \phi \quad \textbf{(4)}$$

where, **τ** is the shear stress on the failure plane,

c is the cohesion of the material,

σ is the normal effective stress on the failure surface, and

ø is the angle of internal friction.

The concept of *Mohr circle* can be used to express the criterion in terms of principal stress;

$$\frac{\sigma_1 - \sigma_2}{2} = \frac{\sigma_1 + \sigma_2}{2} \sin\phi + C\cos\phi \quad \textbf{(5)}$$

where, σ_1 and σ_3 are the major and minor principal stresses, respectively. Equation (5) represents an irregular hexagonal pyramid in the stress space. As can been seen in equation (5), the Mohr-Coulomb criterion ignores the effect of intermediate principal stress. Therefore, it is in convenient to express the Mohr-Coulomb criterion in terms of general three dimensional state of stress defined by six component of stress vector. Hence description of Mohr-Coulomb criterion in terms of conventional forms of stress invariants can be used to define failure and yield criterion. The alternative set of invariants includes a quantity **θ** defined as:

$$\theta = -\frac{1}{3}\sin^{-1}\left[-\frac{3\sqrt{3}}{2}\frac{J_{3D}}{J_{2D}^{3/2}}\right] \quad \textbf{(6)}$$

in addition:

$$-\frac{\pi}{6} \le \theta \le \frac{\pi}{6}$$

where, $\mathbf{J_{2D}}$and $\mathbf{J_{3D}}$ are invariants of the deviatoric stress tensor. The alternative set of invariants $\mathbf{J_1}$, $\mathbf{J_2}$and **θ** could be used in expressing the Mohr-Coulomb criterion conveniently in a three dimensional stress space as:

$$F = J_1 \sin\phi + \sqrt{J_{2D}}\cos\theta - \frac{\sqrt{J_{2D}}}{3}\sin\phi\sin\theta - C\cos\phi = 0 \quad \textbf{(7)}$$

5. Plastic Flow Behavior:

Plastic flow or plastic deformation occurs when the state of stress in the material reaches the yield criterion ***F***. In the theory of plasticity the direction of plastic strain vectors is defined through a flow rule by assuming the existence of a plastic potential function, to which the incremental strain vectors are orthogonal. Then the increment of the plastic strain can be expressed as:

$$d\varepsilon_{ij}^{p} = \lambda \frac{\partial Q}{\partial \sigma_{ij}} \quad \textbf{(8)}$$

Equation (8) are referred to as the Prandtl-Reuss flow rule, where ***Q*** is the plastic potential function, and

λ isa positive scalar vector of proportionality. In the case of frictional material nonassociated flow rule has been preferred. The plastic potential function ***Q*** is often geometrically similar to the failure function ***F*** but with friction angle ***Ø***replaced by dilation angle ***ψ***.

6. Material Nonlinearity:

The material nonlinearity has been introduced using constant stiffness approach, by iteratively modifying the right hand side “load vector”. The global stiffness matrix in such an analysis is formed one time only. Each iteration represents an elastic analysis. Convergence is said to be occurred when stresses generated by the loads satisfy stress-strain law, yield or failure criterion within prescribed tolerance. The load vector at each iteration consists of externally applied loads and self equilibrating “body load”. The body loads have the effect of redistribution stresses within the system, but as they are self equilibrating, they does not alter the net loading on the system.

6.1 Visco-Plasticity:

In this method, the material is allowed to sustain stress as outside the failure criterion for finite "periods” (Zienkiewiez and Cormeau, 1974). Instead of plastic strains, visco-plastic strains are referred to and these are generated at a rate that is related to the amount by which yield has been violated through the expression:

$$\dot{\zeta}^{vp} = F \frac{\partial Q}{\partial \sigma} \quad \textbf{(9)}$$

Multiplication of the visco-plastic strain rate by a pseudo-time step given in an increment of visco-plastic strain is accumulated from one “time step” or iteration to the next. Thus:-

$$\left(\delta\zeta^{vp}\right)^{i} = \Delta t\left(\dot{\zeta}^{vp}\right)^{i} \quad \textbf{(10)}$$

$$\left(\Delta\zeta^{vp}\right)^{i} = \left(\Delta\zeta^{vp}\right)^{i-1} + \left(\delta\zeta^{vp}\right)^{i} \textbf{(11)}$$

The "time step" for *unconditional numerical stability* has been derived by Cormeau (1975) and depends on the assumed failure criterion. Thus, for a *Mohr-Coulomb material* (that has been implemented in the present work):-

$$\Delta t = \frac{4(1+\upsilon)(1-2\upsilon)}{E\left(1-2\upsilon+\sin^2\phi\right)} \textbf{(12)}$$

The derivatives of the *plastic potential function*, ***Q***, with respect to stresses are conveniently expressed through the *chain rule*, thus:-

$$\frac{\partial Q}{\partial \sigma} = \frac{\partial Q}{\partial \sigma_m}\frac{\partial \sigma_m}{\partial \sigma} + \frac{\partial Q}{\partial J_2}\frac{\partial J_2}{\partial \sigma} + \frac{\partial Q}{\partial J_3}\frac{\partial J_3}{\partial \sigma} \textbf{(13)}$$

where $\boldsymbol{J_2=1/2t^2}$ and the visco-plastic strain rate given by equation (9) is evaluated numerically by an expression of the form:-

$$\dot{\zeta}^{vp} = F\left(DQ1M^1 + DQ2M^2 + DQ3M^3\right)\sigma \textbf{(14)}$$

where***DQ1***, ***DQ2***, and ***DQ3*** are scalars equal to $\partial Q/\partial\sigma_m$, $\partial Q/\partial J$ and $\partial Q/\partial J_3$, respectively, and $M^1\sigma, M^2\sigma$ and $M^3\sigma$ are vectors representing $\partial\sigma_m/\partial\sigma$, $\partial J_m/\partial\sigma$ and $\partial J_3/\partial\sigma$, respectively. This is essentially the same notation used by Zienkiewicz (1991).

The body-loads $\boldsymbol{P_b^i}$ are accumulated at each "time step" within each load step by assuming the following integrals for all elements containing a yielding *Gauss point*:-

$$P_b^i = P_b^{i-1} + \sum_{element}^{all}\int B^T D^e\left(\delta\zeta^{vp}\right)^i d(element) \textbf{(15)}$$

This process is repeated at each (time step) iteration until no Gauss point stresses violate the failure criterion to within a certain tolerance. The convergence criterion is based on a dimensionless measure of the amount by which the displacement increment vector $\boldsymbol{\delta^i}$ changes from one iteration to the next.

7. Interface Modeling:

Thin layer interface element developed by Desai et. al. (1984), has been used in this work to represent the interface modeling between the pile and the raft materials and soil material. The constitutive matrix can be given by (Desai et al, 1984) :

$$[C]_i = \begin{bmatrix} [C_{nn}]_i & [C_{ns}]_i \\ [C_{sn}]_i & [C_{ss}]_i \end{bmatrix} \quad \textbf{(16)}$$

where, **[C]** constitutive matrix,

$[C_{nn}]$ normal component, and

$[C_{ns}]$, $[C_{sn}]$ coupling effect.

Since it is difficult to determine the coupling terms from laboratory tests, they are not included herein. The development of the stiffness characteristics of thin layer interface element follows essentially the same procedure as solid element. For linear elastic behaviour constitutive matrix can be expressed as (Desai et al, 1984):

$$[C^e] = \begin{bmatrix} C_1 & C_2 & C_2 & 0 & 0 & 0 \\ C_2 & C_1 & C_2 & 0 & 0 & 0 \\ C_2 & C_2 & C_1 & 0 & 0 & 0 \\ 0 & 0 & 0 & G_{i1} & 0 & 0 \\ 0 & 0 & 0 & 0 & G_{i2} & 0 \\ 0 & 0 & 0 & 0 & 0 & G_{i3} \end{bmatrix} = \begin{bmatrix} [C_n]_i & 0 \\ 0 & [C_s]_i \end{bmatrix} \quad \textbf{(17)}$$

where, $C_1 = \dfrac{E(1-v)}{(1+v)(1-2v)}$, $C_2 = \dfrac{Ev}{(1+v)(1-2v)}$,

E elastic Young modulus,

v Poisson's ratio, and

G_{ii} (i=1,2,3) shear modulus.

Here, it is assumed that the shear response is uncoupled from the normal response represented by $[C_n]$.

The elastic constitutive matrix has been used here in to describe Elasto-plastic (nonlinearity) behaviour of thin layer interface element by using the constant stiffness iteration approach in which nonlinearity is introduced by iteratively modifying the right hand side "load vector".

8. Numerical Algorithm:

A computer program was developed (Al-Baghdadi, 2006) using FORTRAN 90 programming language to solve the equilibrium equations of the finite element modeling for the piled-raft system. The program can analyze two or more types of materials.

9. Verification of Algorithm:

Verifications of developed algorithm have been made by comparing its results with experimental findings from similar models. Figures (1) and (2) shows a comparison between the experimental and numerical results for piled-raft models in clay, experimental results have been produced by Wiesner and Brown (1980).Two methods have been used for representing the undrained condition one by using Poisson's ratio close to (0.5) and other by adding the bulk modulus of water to constitutive matrix of soil in compression locations (Smith and Griffiths, 1998). The results indicate very good agreement between the numerical and experimental results.

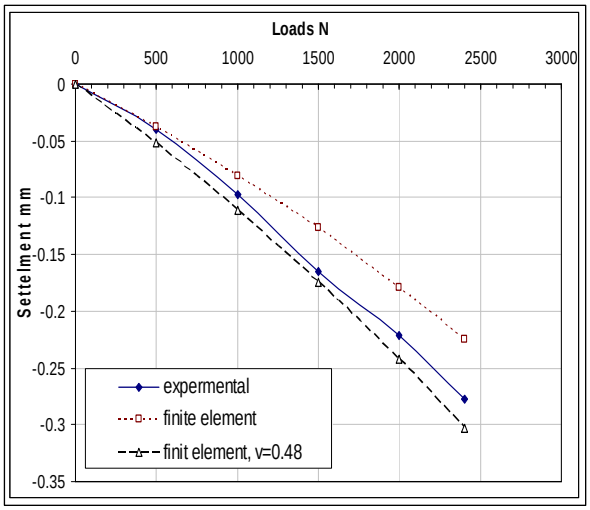

Figure (1) Load –settlement curves for the square piled raft model.

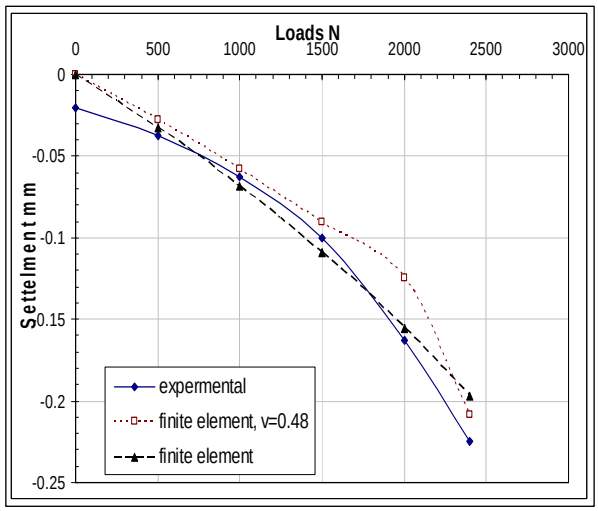

Figure (2) Load –settlement curves for the rectangular piled raft model.

10. Parametric Study:

A square piled-raft model in sandy soil is analyzed to investigate the influence of various parameters on the settlement and differential settlement. The parameters are pile length, pile spacing, pile diameter, number of piles and thickness of the raft. The dimensions of the raft are (10X10 m). Soil extent from both sides of the piled raft model has been taken as five times as the raft width or length (Reul and Randolph, 2002), the properties of the soil are given Table (1). The properties of the piled raft and the finite element mesh used are listed in Tables (2) and (3); respectively.Figure (3) shows the locations and magnitudes of applied loads, they represent the columns reactions. The use of uniformly distributed loading over the raft area may be adequate for the preliminary stage. They may not be so when considering in more details where piles should be located upon introducing column loadings (Poulos, 2001). One quarter of the model has been analyzed because of symmetry. The investigations are based on settlement ratio. It can be defined as follows:

Settlement Ratio= [Settlement of piled raft / Settlement of adjacent raft] (10)

The differential settlement ratio can be calculated by :

Differential Settlement = [Settlement at Center- Settlement at Corner] (11)

Table (1) Soil parameters of the piled raft model.

Parameter	Value
Depth of soil layer	30 m
Extent of soil layer for X and Y directions	10 m
Angle of internal friction (Ø)	36.5 degree
Angle of dilation (ψ)	11.4 degree
Angle of friction between soil and concrete	16 degree
Cohesion (C)	0 kN/m^2
Modulus of elasticity (E)	$0.96*10^5$ kN/m^2
Poisson's ratio (ν)	0.28
Unit weigh (γ)	16 kN/m^3
Lateral earth pressure coefficient at rest (K_o)	0.405

Table (2) Concrete parameter of the piled raft model.

Parameter	Value
Raft length	10m
Raft width	10m
Raft thickness	0.5m
Pile length	25m
Pile diameter	0.637m
Modulus of elasticity (E)	$2.2*10^7$ kN/m^2
Poisson's ratio (ν)	0.3
Unit weigh (γ)	24 kN/m^2

Table (3) Properties of the finite element mesh.

Parameter	Value
Number of total elements	4693
Number of columns in X direction	19
Number of columns in Y direction	19
Number of columns in Z direction	13
Number of integration points per element	27
Number of nodes per element	20

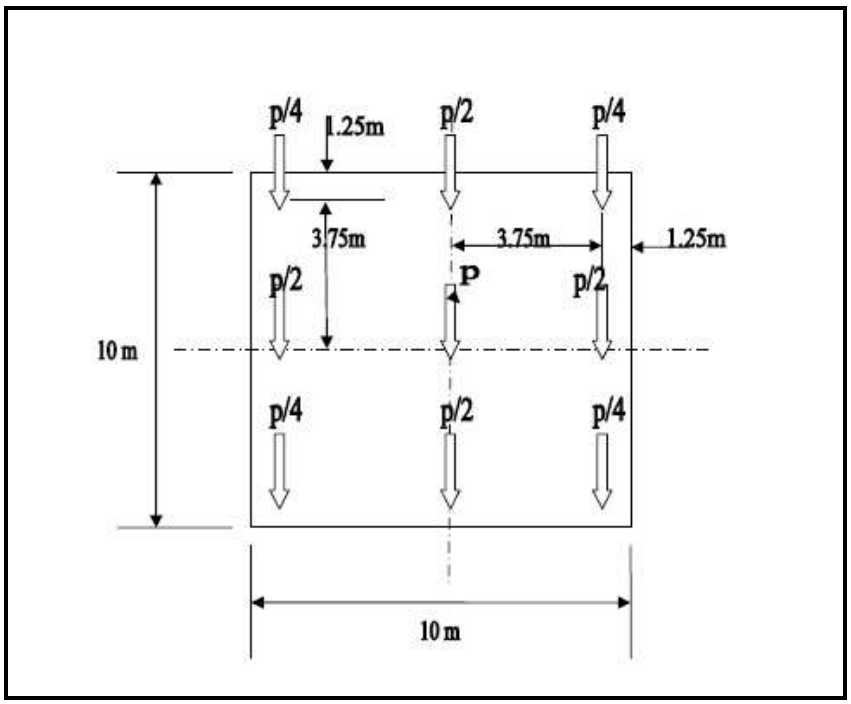

Figure (3) Locations and magnitude of applied loads on the piled raft model.

10.1 Influence of Pile Length on Piled-Raft Settlement:

The piled-raft model with nine piles as shown in Figure (4) has been tested. The length of the piles varies from (5m) to (25m). Numerical results are shown in Figures (5) and (6). They show that the increase in pile length decrease the settlement ratio for both central and differential cases. In addition, it indicates that the load increment has little or no effect on the settlement ratio. For this reason, it is possible to draw the effect of the pile length on settlement ratio for some loading, say, (50000 kN) as shown in Figure (7) and (8). They indicate that (55%) of the settlement reduction can be reached with pile length over depth of the soillayer ratio (L/D) more than (0.8). The relation between settlement ratio and pile length over raft width ratio (L/W) can give good indication for selecting the length of the pile for preliminary design purposes.

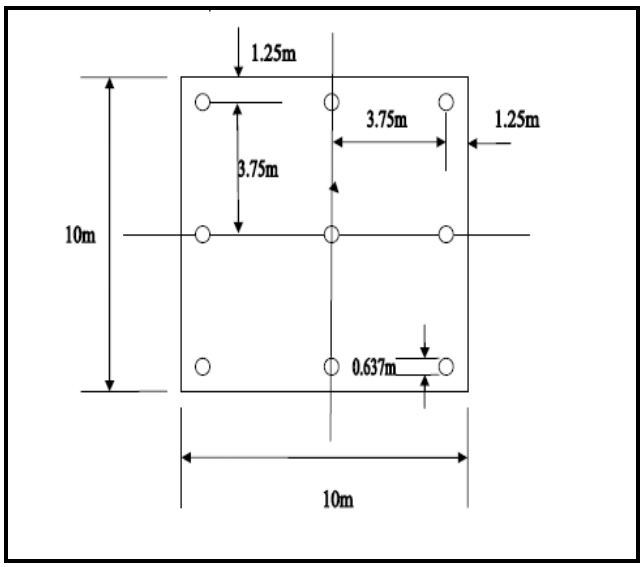

Figure (4) Locations of nine piles of a piled raft model.

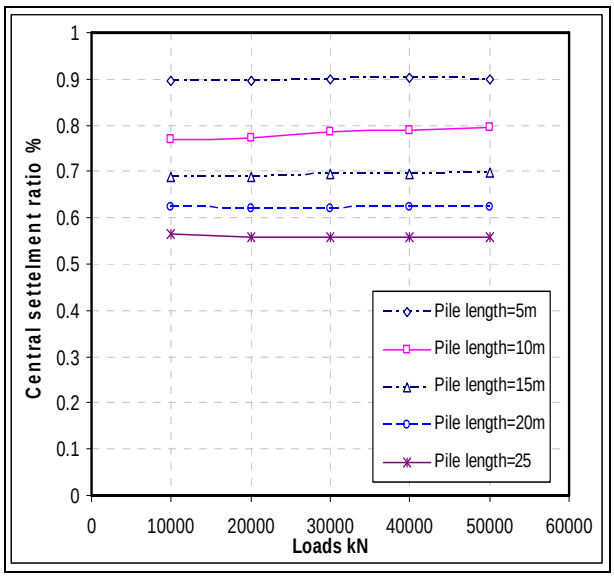

Figure (5) Effect of pile length on central settlement ratio.

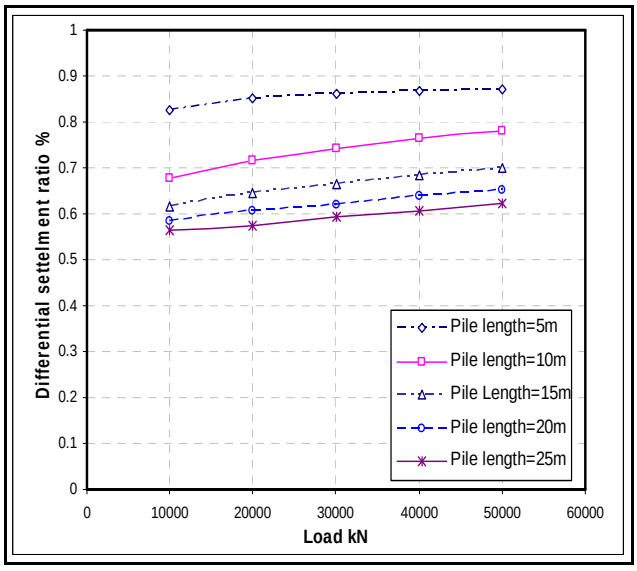

Figure (6) Effect of pile length on differential settlement ratio.

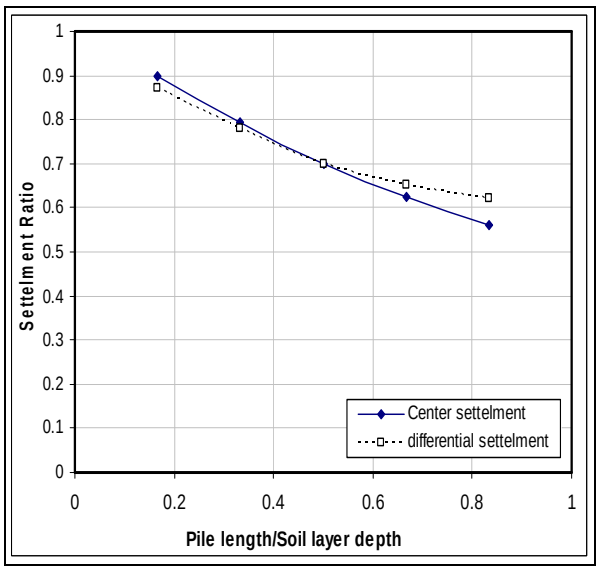

Figure (7) Effect of length over depth ratio on settlement ratio for (50000 kN).

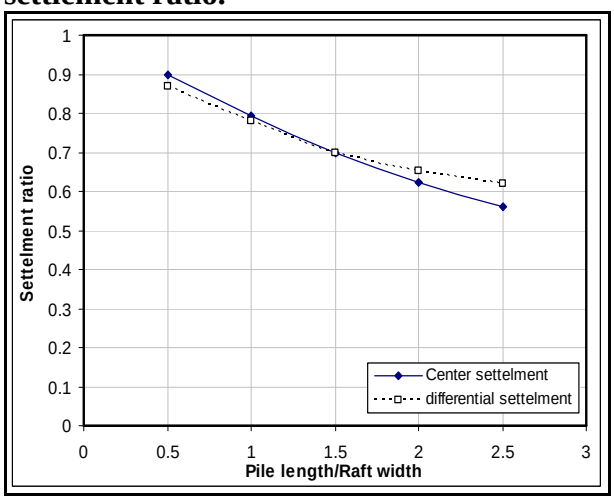

Figure (8) Effect of length over width ratio on settlement ratio for (50000 kN).

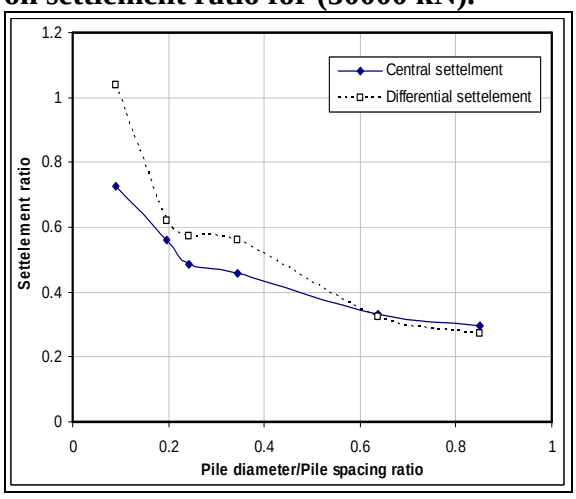

Figure (9) Effect of diameter over spacing ratio on settlement ratio for (50000 kN).

10.2 Influence of Pile Spacing on Piled- Raft Settlement:

Figure (9) shows clearly the effect of pile spacing on settlement ratio. The relation between the pile diameter over pile spacing ratio (D/S) and settlement ratio has been drawn. The settlement ratio, when the D/S ratio increased, (70%) of settlement reduction can be reached with D/S ratio exceeding (0.6). When the D/S ratio reaches (0.8), there is very small effect on settlement ratio, because at this percentage, the soil between piles begins to work with piles like one block, and no slip will occur between pile and the surrounding soil.

10.3 Influence of Pile Diameter on Piled- Raft Settlement:

A variable pile diameter (0.637m-1.91m) has been used. Figures (10) and (11) show the effect of pile diameter on reducing settlement of piled-raft footings. With pile diameter equals to (1.91m), both central and differential settlements can be reduced by (70%) and (74%), respectively. However it can be reduced by (55%) with pile diameter equals to (0.637m).

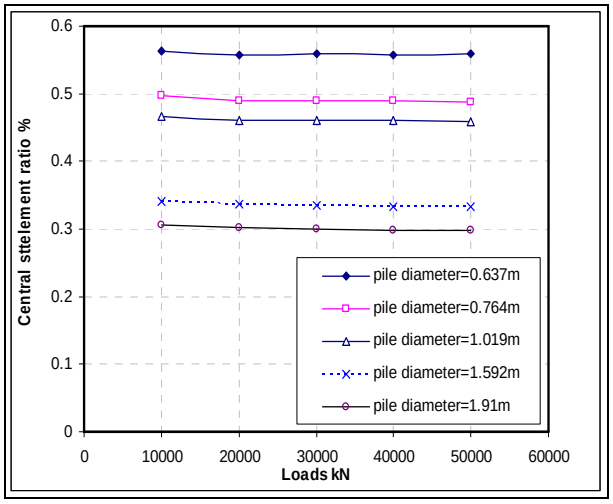

Figure (10) Effect of pile diameter on central settlement ratio.

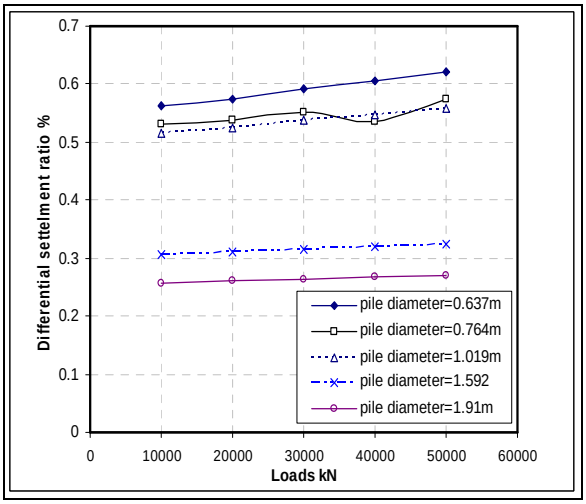

Figure (11) Effect of pile diameter on differential settlement ratio.

10.4 Influence of Pile Numbers on Piled- Raft Settlement:

The same piled-raft model has been used with a variable number of piles which ranges from (4) to (9) piles. Figure (12) shows the locations of piles. Figures (13) and (14) show the effect of number of piles on the settlement ratio in center and differential cases, respectively. As seen in Figures (13) and (14), four piles at corners can reduce the central settlement more than (25%), but it increased the differential one by (4%) under (50000 kN). Additional two piles located at edges have no effect, but two additional piles symmetrical in locations make the last four piles effect in reducing settlement by (20%) for differential and (10%) for the central one. Figure (15) shows that clearly.

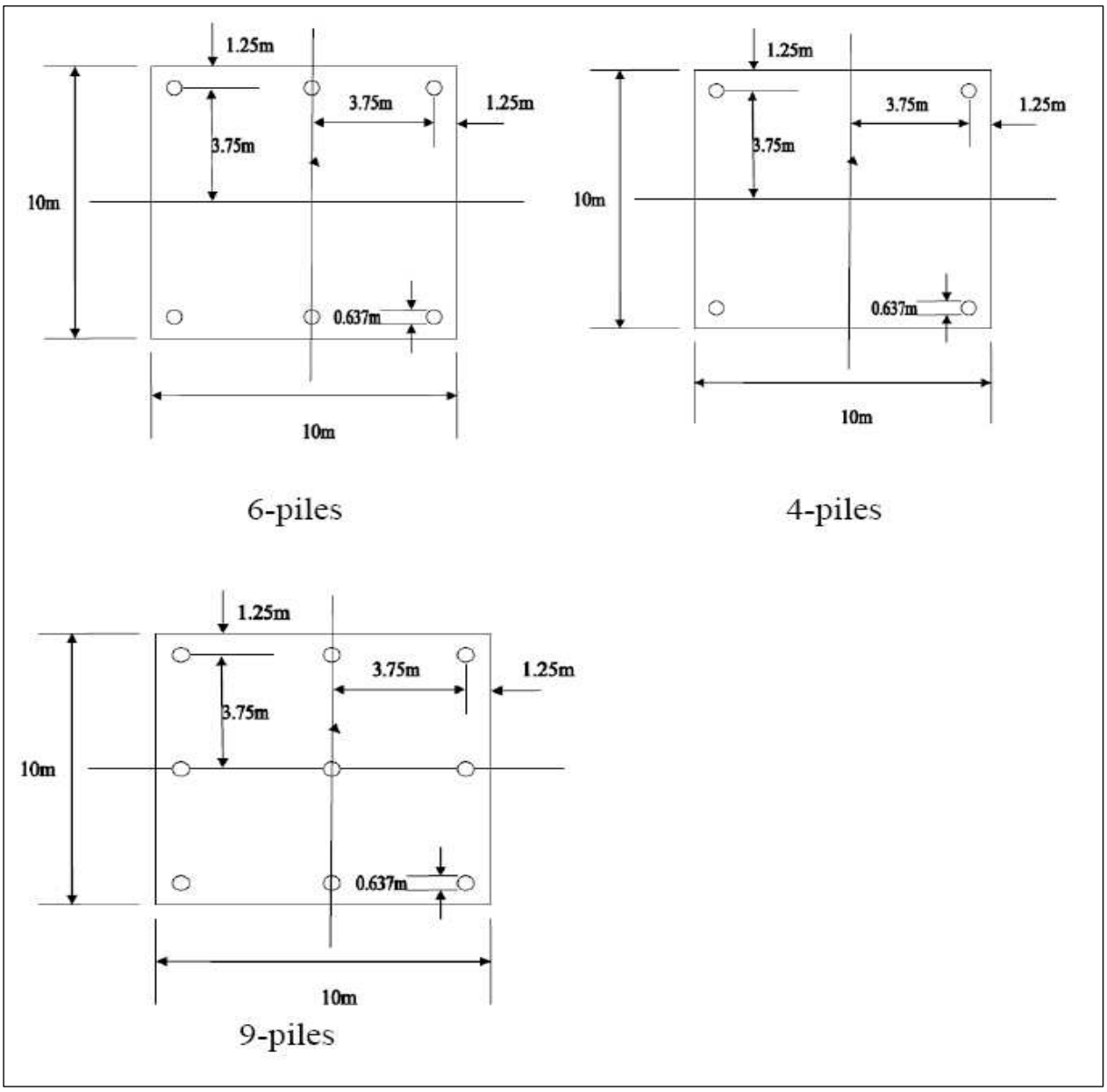

Figure (12) Locations of piles in the piled-raft model.

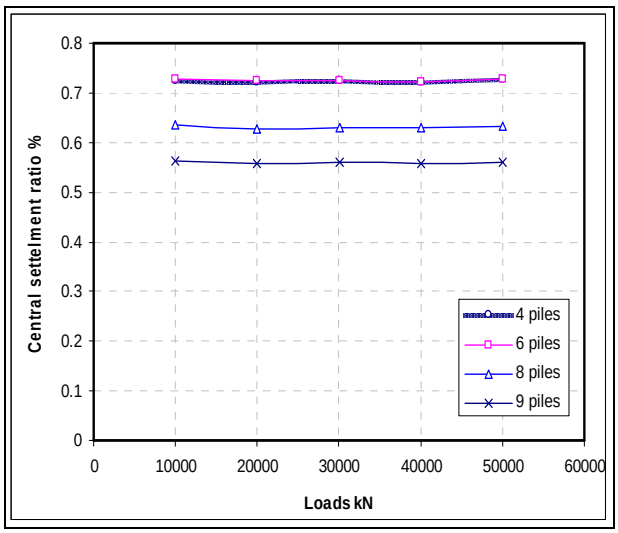

Figure (13) Effect of pile number on central settlement ratio

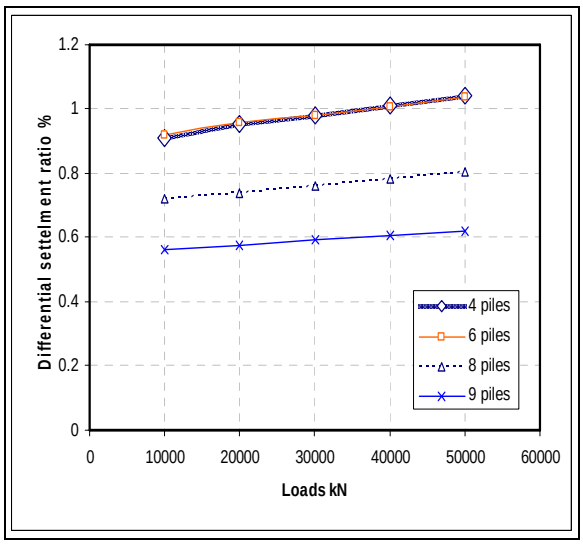

Figure (14) Effect of pile number on differential settlement ratio.

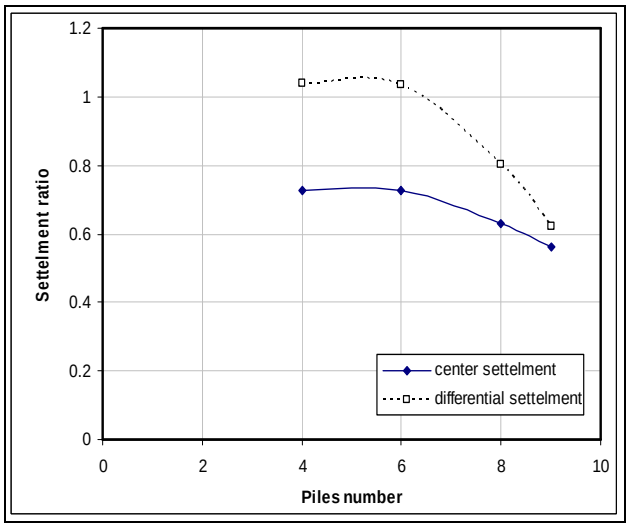

Figure (15) Effect of pile number on settlement ratio.

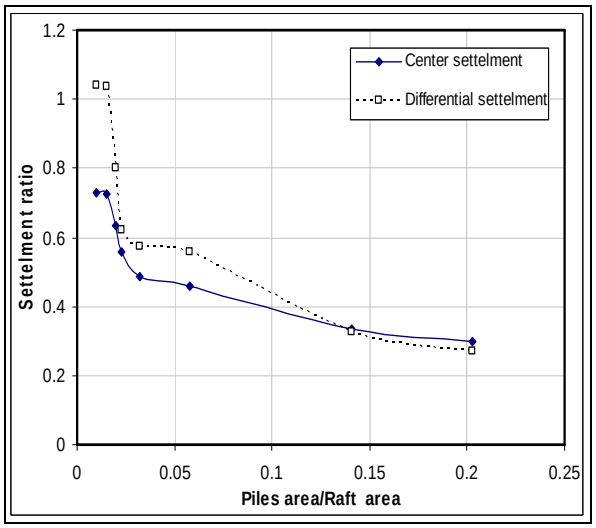

Figure (16) Effect of (piles area/raft area) ratio on settlement ratio.

10.5 Influence of Pile Area on Piled- Raft Settlement:

The total area of piles as related with three previous parameters, namely, pile number, pile diameter, and pile spacing is studied here. Figure (16) shows the effect of piles area over raft area ratio (A_p/A_r) on the settlement ratio regardless on the locations of the piles. (75%) of settlement reduction can be obtained with (A_p/A_r) between (0.15-0.2).

10.6 Influence of Raft Thickness on Piled- Raft Settlement:

The influence of raft thickness variation on settlement ratio has been investigated by using the same model of the piled-raft with (9) piles and (25m) pile length. To obtain the settlement ratio, a similar model of raft foundation with same thickness and conditions has been adopted. As seen in Figures (17), (18) and (19), the improvement of differential settlement by adding piles is more effective

when the ratio between raft thickness and raft width is smaller than (0.1). For central settlement, raft thickness has a very small influence on settlement ratio.

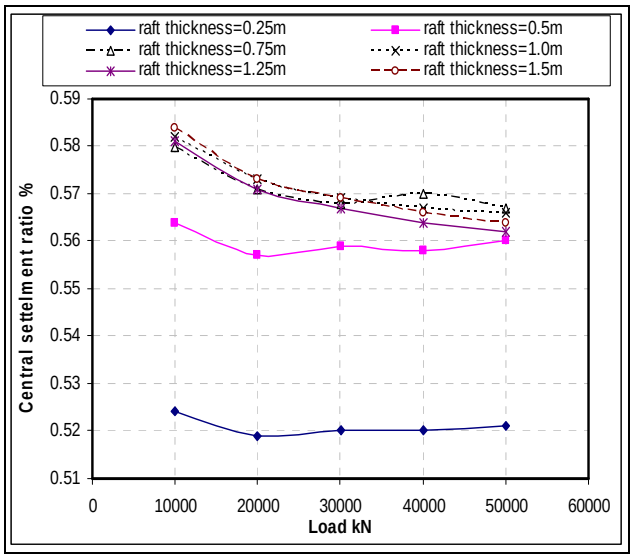

Figure (17) Effect of raft thickness on central settlement ratio.

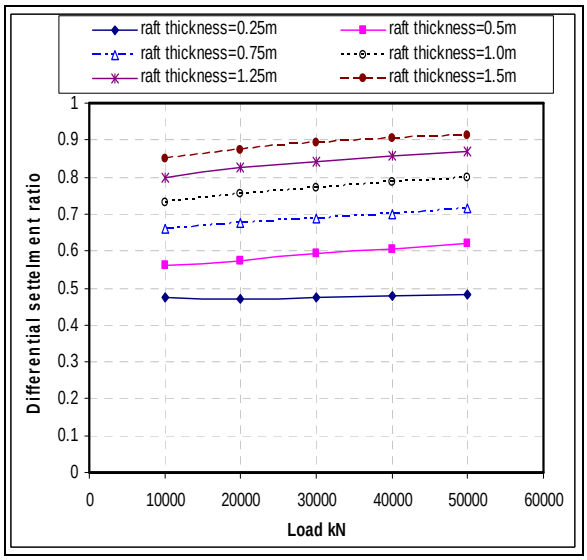

Figure (18) Effect of raft thickness on differential settlement ratio.

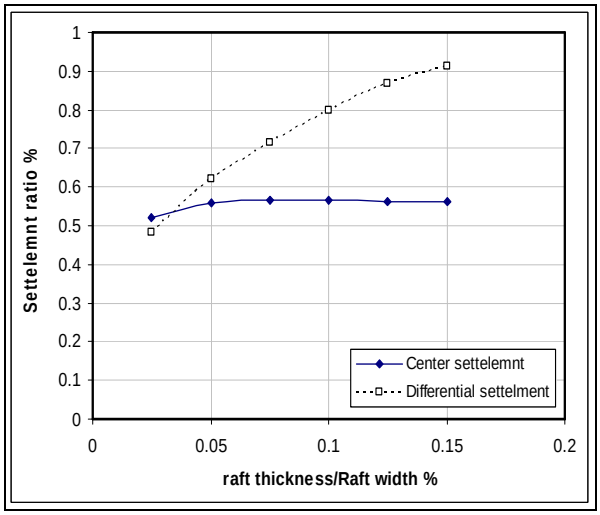

Figure (19) Effect of (raft thickness/raft width) on settlement ratio.

11. Conclusions:

From this investigation, the following points can be drawn:

1. The computer code developed is found to be very useful and can be used for wide range of applications in many soil and soil-structure interaction problems.
2. The three-dimensional nonlinear and linear finite element model, which was adopted in the present work, is suitable for predicting the behavior of a soil-pile-raft system. The numerical results were in good agreement with available experimental load-settlement results throughout the entire range of behaviour.

3. The adoption of a thin layer element to represent the interface modeling is satisfied for small displacement cases.
4. From numerical investigations, the main effective factors on the behavior of a piled-raft foundation were, pile length, pile spacing, pile diameter, number of piles, total piles area, and raft thickness.
5. Pile length has a significant influence in reducing both central and differential settlements. It is observed that it is possible to reduce the settlement more than (40%) with pile length equals to (80%) of soil layer depth.
6. Pile spacing has a major effect in reducing settlement. Maximum settlement reduction can be obtained with (pile diameter/pile spacing) ratio between (0.8-1.0). By this range, the soil between piles works with the piles as a block and no slippage will occur between piles and the surrounding soil.
7. Regardless, the relation between spacing of piles and pile number, the increment of pile number causes a decrement in settlement. To control differential settlement, the locations of the piles have to be selected optimally.
8. Piles/Raft area ratio has a significant effect on reducing settlement, (75%) of settlement reduction can be obtained with a Piles/Raft area ratio in the range of (0.15-0.2).
9. Increasing of raft thickness reduces the effect of adding piles for controlling differential settlement. Raft thickness has a very small effect on reducing settlement ratio for the central settlement.

12. References:

1. Al-Baghdadi N., "Soil-Pile-Raft Analysis by The Finite Element Method", M.Sc. Thesis, College of Engineering, University of Kufa, 2006.
2. Brown P.T. and Wiesner T.J., "The Behaviour of Uniformly Loaded Piled Strip Footings", *Soils and Foundations*, Volume15, No. 4, pp13-21, 1975.
3. Burland J.B., Broms B.B. and de Mello V.F.B., "Behaviour of Foundations and Structures", *Proceedings of the Ninth International Conference of Soil Mechanics and Foundation Engineering*, Tokyo, Volume 2, pp 495-546, 1977.
4. Cormeau I.C., "Numerical Stability in Quasi-Static Elasto-Viscoplasticity", *International Journal in Numerical Methods in Eingineering*, 9 (1), 109-127, 1975.
5. Davis E.H. and Poulos H.G., "The Analysis of Piled Raft Systems", *Australian Geomechanics Journal*, G2: 21-27, 1972.

6. Desai C.S., Zamman M.M., Lightner J.G., and Siriwardane H.J., "Thin Layer Element for Interfaces and Joints', *International Journal of Numerical and Analytical Methods in Geomechanics*, Volume 8, pp19-43, 1984.
7. Franke E., "Measurements beneath Piled Rafts", Keynote Lecture, *ENPC Conference*, Paris, pp1-28, 1991.
8. Franke E., Lutz B. and El-Mossallamy Y., "Measurements and Numerical Modelling of High-RiseBuilding Foundations on Frankfurt Clay", *Geotechnical Special Publication, 40*, ASCE, Volume 2, pp 1325-1336, 1994.
9. Hansbo S., "Interaction Problems Related to the Installation of Pile Groups", *Seminar on Deep Foundations on Bored and Auger Piles*, BAP2, Ghent, pp59-66, 1993.
10. Hooper J.A., "Observations on the Behaviour of a Piled-Raft Foundation on London Clay", *Proceeding of the Institution Civil Engineers*, Volume 55, No.2, pp855-877, 1973.
11. Poulos H.G., "Methods of Analysis of Piled Raft Foundations" A Report Prepared on Behalf of Technical Committee TC18 on Piled Foundations, *International Society of Soil Mechanics and Geotechnical Engineering*, 2001.
12. Price G. and Wardle I.F., "Monitoring of Load Sharing Between Piles and Raft", Queen Elizabeth II Conference Centre, *Proceedings of the Institution of Civil Engineers*, Volume 80, No.1, pp1505-1518, 1986.
13. Reul O. and Randolph M. F., "Piled Rafts in Overconsolidated Clay: Comparison of in situ Measurements and Numerical Analysis", *Geotechnique*, volume 53, No. 3, pp301-315, 2003.
14. Smith I. M. and Griffiths D.V., "Programming the Finite Element Method", John Wiley, U.K., 1998.
15. Sommer H., Wittmann P. and Ripper P., "Piled Raft Foundation of a Tall Building in Frankfurt Clay", *Proceedings of the Eleventh International Conference of Soil Mechanics and Foundation Engineering*, San Francisco, Volume 4: pp2253-2257, 1985.
16. Timoshenko S. and Goodier J.N.," Theory of Elasticity", 2nd edition, McGraw-Hill, USA, 1951.
17. Wiesner T.J. and Brown P.T., "Laboratory Test on Model Piled Raft Foundations", *Journal of the Geotechnical Engineering Division, ASCE*, Volume 106, No. GT7, July, 1980.
18. Zeevaert L., "Compensated Friction-Pile Foundation to Reduce the Settlement of Buildings on Highly Compressible Volcanic Clay of Mexico City", *Proceedings of the Fourth*

International Conference of Soil Mechanics and Foundation Engineering, London, Volume 2, 1957.

19. Zienkiewicz O.C., "The Finite Element Method in Engineering Science", McGraw-Hill, U.K., 1971.
20. Zienkiewicz O.C. and Cormeau I.C., "Viscoplasticity, Plasticity and Creep in Elastic Solids A Unified Numerical Solution Approach", *International Journal for Numerical Methods in Engineering*, Volume 8, pp821-845, 1974.
21. Zienkiewicz O.C., "The Finite Element Method", 4th edition, McGraw-Hill, New York, 1991.